



Full and semi-analytic analyses of two-pump parametric amplification with pump depletion

Steffensen, Henrik; Ott, Johan Raunkjær; Rottwitt, Karsten; McKinstrie, C.J.

Published in:
Optics Express

Link to article, DOI:
[10.1364/OE.19.006648](https://doi.org/10.1364/OE.19.006648)

Publication date:
2011

Document Version
Publisher's PDF, also known as Version of record

[Link back to DTU Orbit](#)

Citation (APA):
Steffensen, H., Ott, J. R., Rottwitt, K., & McKinstrie, C. J. (2011). Full and semi-analytic analyses of two-pump parametric amplification with pump depletion. *Optics Express*, 19(7), 6648-6656.
<https://doi.org/10.1364/OE.19.006648>

General rights

Copyright and moral rights for the publications made accessible in the public portal are retained by the authors and/or other copyright owners and it is a condition of accessing publications that users recognise and abide by the legal requirements associated with these rights.

- Users may download and print one copy of any publication from the public portal for the purpose of private study or research.
- You may not further distribute the material or use it for any profit-making activity or commercial gain
- You may freely distribute the URL identifying the publication in the public portal

If you believe that this document breaches copyright please contact us providing details, and we will remove access to the work immediately and investigate your claim.

Full and semi-analytic analyses of two-pump parametric amplification with pump depletion

H. Steffensen,^{1,*} J. R. Ott,¹ K. Rottwitt,¹ and C. J. McKinstrie²

¹*Department of Photonics Engineering, Technical University of Denmark,
2800 Lyngby, Denmark*

²*Bell Laboratories, Alcatel-Lucent, Holmdel, New Jersey 07733, USA*

[*hste@fotonik.dtu.dk](mailto:hste@fotonik.dtu.dk)

Abstract: This paper solves the four coupled equations describing non-degenerate four-wave mixing, with the focus on amplifying a signal in a fiber optical parametric amplifier (FOPA). Based on the full analytic solution, a simple approximate solution describing the gain is developed. The advantage of this new approximation is that it includes the depletion of the pumps, which is lacking in the usual quasi-linearized approximation. With the proposed model it is thus simple to predict the gain of a FOPA, which we demonstrate with a highly nonlinear fiber to show that an undepleted FOPA can produce a flat gain spectrum with a bandwidth in the 100-nm range, centered on the zero-dispersion wavelength. When running the FOPA in depletion, this range can be slightly increased.

© 2011 Optical Society of America

OCIS codes: (060.2320) Fiber optics amplifiers and oscillators; (060.2330) Fiber optics communications; (190.4370) Nonlinear optics, fibers.

References and links

1. J. Hansryd, P. A. Andrekson, M. Westlund, J. Li, and P.-O. Hedekvist, "Fiber-based optical parametric amplifiers and their applications," *IEEE J. Sel. Top. Quantum Electron.* **8**, 506–520 (2002).
2. M. E. Marhic, *Fiber Optical Parametric Amplifiers, Oscillators and Related Devices* (Cambridge University Press, 2007).
3. R. Slavík, F. Parmigiani, J. Kakande, C. Lundström, M. Sjödin, P. A. Andrekson, R. Weerasuriya, S. Sygletos, A. D. Ellis, L. Grüner-Nielsen, D. Jakobsen, S. Herstrøm, R. Phelan, J. O’Gorman, A. Bogris, D. Syvridis, S. Dasgupta, P. Petropoulos, and D. J. Richardson, "All-optical phase and amplitude regenerator for next-generation telecommunications systems," *Nat. Photonics* **4**, 690–695 (2010).
4. C.-S. Brès, A. Wiberg, B. P.-P. Kuo, N. Alic, and S. Radic, "Multicasting of 320-Gb/s Channel in Self-Seeded Parametric Amplifier," *IEEE Photon. Technol. Lett.* **21**, 1002–1004 (2009).
5. S. Radic, C. J. McKinstrie, R. M. Jopson, J. C. Centanni, and A. R. Chraplyvy, "All-optical regeneration in one- and two-pump parametric amplifiers using highly nonlinear optical fiber," *IEEE Photon. Technol. Lett.* **15**, 957–959 (2003).
6. C. Peucheret, M. Lorenzen, J. Seoane, D. Noordegraaf, C. V. Nielsen, K. Rottwitt, and L. Grüner-Nielsen, "Amplitude regeneration of RZ-DPSK signals in single-pump fiber-optic parametric amplifiers," *IEEE Photon. Technol. Lett.* **21**, 872–874 (2009).
7. J. Kakande, F. Parmigiani, R. Slavík, L. Grüner-Nielsen, D. Jakobsen, S. Herstrøm, P. Petropoulos, and D. J. Richardson, "Saturation effect in degenerate phase sensitive fiber optic parametric amplifiers," *ECOC*, paper Th.10.C.2 (2010).
8. M. N. Islam and O. Boyraz, "Fiber parametric amplifiers for wavelength band conversion," *IEEE J. Sel. Top. Quantum Electron.* **8**, 527–537 (2002).
9. J. M. Chávez Boggio, J. R. Windmiller, M. Knutzen, R. Jiang, C. Brès, N. Alic, B. Stossel, K. Rottwitt, and S. Radic, "730-nm optical parametric conversion from near- to short-wave infrared band," *Opt. Express* **16**, 5435–5443 (2008).

10. K. Croussore and G. Li, "Phase regeneration of NRZ-DPSK signals based on symmetric-pump phase-sensitive amplification," *IEEE Photon. Technol. Lett.* **19**, 864–866 (2007).
11. P. Kylemark, H. Sunnerud, M. Karlsson, and P. A. Andrekson, "Semi-analytic saturation theory of fiber optical parametric amplifiers," *J. Lightwave Technol.* **24**, 3471–3479 (2006).
12. Y. Chen and A. W. Snyder, "Four-photon parametric mixing in optical fibers: effect of pump depletion," *Opt. Lett.* **14**, 87–89 (1989).
13. G. Cappelline and S. Trillo, "Third-order three-wave mixing in single-mode fibers: exact solutions and spatial instability effects," *J. Opt. Soc. Am. B* **8**, 824–838 (1990).
14. C. J. McKinstrie, X. D. Cao, and J. S. Li, "Nonlinear detuning of four-wave interactions," *J. Opt. Soc. Am. B* **10**, 1856–1869 (1993).
15. G. P. Agrawal, *Nonlinear Fiber Optics*, 4th Ed. (Elsevier, 2007).
16. K. Inoue, "Polarization effect on four-wave mixing efficiency in a single-mode fiber," *IEEE J. Quantum Electron.* **28**, 883–894 (1992).
17. C. J. McKinstrie, H. Kogelnik, R. M. Jopson, S. Radic, and A. V. Kanaev, "Four-wave mixing in fibers with random birefringence," *Opt. Express* **12**, 2033–2055 (2004).
18. J. M. Manley and H. E. Rowe, "Some general properties of nonlinear elements—Part I. General energy relations," *Proc. IRE* **44**, 904–913 (1956).
19. M. T. Weiss, "Quantum derivation of energy relations analogous to those for nonlinear reactances," *Proc. IRE* **45**, 1012–1013 (1957).
20. P. F. Byrd and M. D. Friedman, *Handbook of Elliptic Integrals for Engineers and Physicists* (Springer, 1954).
21. M. Hirano, T. Nakanishi, T. Okuno, and M. Onishi, "Silica-based highly nonlinear fibers and their application," *IEEE J. Sel. Top. Quantum Electron.* **15**, 103–113 (2009).
22. C. J. McKinstrie and M. G. Raymer, "Four-wave-mixing cascades near the zero-dispersion frequency," *Opt. Express* **14**, 9600–9610 (2006).

1. Introduction

Lately, fiber-optical parametric amplifiers (FOPAs) have attracted significant attention. There are several reasons for this, including their ability to provide phase-sensitive amplification [1–3], multicasting [4], regeneration [3, 5–7] and wavelength conversion [8, 9]. It is noted that especially when applying the FOPA as an amplifier or regenerator, most emphasis has been on single-pumped amplifiers. However research on phase-sensitive amplification is often based on dual-pumped amplifiers [3, 10].

In wavelength conversion as well as in regeneration, amplifier saturation is of particular importance. Consequently, it is essential to understand and to be able to predict the depletion behavior of FOPA's. Until now, the focus has been on single-pumped FOPAs. However, in this work we consider depletion in dual-pumped FOPAs.

Previously Kylemark *et al.* [11] derived an approximation for a single-pumped FOPA operated at the specific phase mismatch which allows for total conversion of power from the pump. Their approach is based on selecting a specific phase matching condition where the coupling of power is only directed from the pump to the signal. Other phase matching conditions result in periodic coupling of the power between pump and signal, and are not treated. In this work we adopt a similar approach, though for a dual-pumped FOPA. In addition, we extend the approach to any phase mismatch by neglecting the periodic behavior of the power flow. Depletion and the periodic behavior of the flow of power have previously been described analytically by the use of Jacobi elliptic functions [12–14]. In this work we derive a simpler analytical model of saturated dual-pumped FOPA. This model provides a useful tool to understand and design a two-pump FOPA operated in saturation, as for example when designing a wideband regenerator based on operating the amplifier in depletion. The application of the model presented in this work is discussed with a focus on optimizing the bandwidth of a two-pump parametric amplifier. By locating the pumps symmetrically around the zero-dispersion wavelength (ZDW), a bandwidth in the 100-nm range is achievable.

2. Theory

In general we consider an electric field consisting of four continuous waves (CWs), at frequencies ω_1 through ω_4 . In non-degenerate four-wave mixing (FWM), the four distinct waves interact with each other under the condition $\omega_1 + \omega_4 = \omega_2 + \omega_3$. Two of these, numbers 2 and 3, are in this paper used as pumps, while 1 is a signal, also denoted s , that is to be amplified, and 4 is the idler, i , that arises when the signal is amplified. Under the assumption that the four waves are sufficiently separated in frequency, the nonlinear Schrödinger equation (NLS) can be reduced to four coupled differential equations for the complex field amplitudes [15]:

$$\frac{dA_1}{dz} = i\beta_1 A_1 + i\gamma \{ [|A_1|^2 + 2(|A_2|^2 + |A_3|^2 + |A_4|^2)] A_1 + 2A_2 A_3 A_4^* \}, \quad (1a)$$

$$\frac{dA_2}{dz} = i\beta_2 A_2 + i\gamma \{ [|A_2|^2 + 2(|A_1|^2 + |A_3|^2 + |A_4|^2)] A_2 + 2A_1 A_3^* A_4 \}, \quad (1b)$$

$$\frac{dA_3}{dz} = i\beta_3 A_3 + i\gamma \{ [|A_3|^2 + 2(|A_1|^2 + |A_2|^2 + |A_4|^2)] A_3 + 2A_1 A_2^* A_4 \}, \quad (1c)$$

$$\frac{dA_4}{dz} = i\beta_4 A_4 + i\gamma \{ [|A_4|^2 + 2(|A_1|^2 + |A_2|^2 + |A_3|^2)] A_4 + 2A_1^* A_2 A_3 \}, \quad (1d)$$

where γ is the nonlinear strength, β_α is the wave-number and the index α may be either 1, 2, 3 or 4. It is assumed that the input fields are parallel polarized, but in the case of perpendicular pumps and sidebands, the factor of 2 in the coupling term should be changed to a 1 [16, 17]. The most common method of solving Eq. (1) is by assuming that the pump powers remain much greater than the signal and idler power at all times and that the power loss of the pumps is negligible [1]. This will quasi-linearize the differential equations and for pumps with identical power, P_p , result in

$$P_s(z) = P_s(0) \left\{ 1 + \left[\frac{2\gamma P_p}{g} \sinh(gz) \right]^2 \right\}, \quad (2)$$

$$P_i(z) = P_s(0) \left[\frac{2\gamma P_p}{g} \sinh(gz) \right]^2, \quad (3)$$

where $g^2 = (2\gamma P_p)^2 - (\kappa/2)^2$ and $\kappa = 2\gamma P_p + \Delta\beta$. $\Delta\beta$ is the wave-number mismatch given as $\Delta\beta = \beta_1 - \beta_2 - \beta_3 + \beta_4$, and since P_p is the pump power in each pump and these are assumed identical, the expression resembles the expression known from single-pumped parametric amplifiers [1]. Generally, gain exists when $-6\gamma P_p < \Delta\beta < 2\gamma P_p$, but the greatest gain, $G(z) = P_s(z)/P_s(0)$, is obtained with $\kappa = 0$, thus requiring that $\Delta\beta = -2\gamma P_p$. This condition effectively means that the self- and cross-phase-modulation and dispersion induced wave-number shifts cancel each other. However as the pumps are depleted, the effective wave-number mismatch, κ , will change and thus decrease the coupling efficiency. The problem with this solution is that it does not account for pump depletion and nonlinear detuning.

By rewriting the complex amplitude A in Eq. (1) in terms of the real variables, power P and phase ϕ , as $A_\alpha = \sqrt{P_\alpha} \exp i\phi_\alpha$, the differential equations are instead written as

$$\frac{dP_\alpha}{dz} = s_\alpha 4\gamma \sqrt{\prod_\beta P_\beta} \sin \theta, \quad (4)$$

$$\frac{d\phi_\alpha}{dz} = \beta_\alpha + \gamma (2 \sum_\beta P_\beta - P_\alpha) + 2\gamma \frac{\sqrt{\prod_\beta P_\beta}}{P_\alpha} \cos \theta, \quad (5)$$

where $\theta = \phi_1 + \phi_4 - \phi_2 - \phi_3$ and $s_\alpha = d\theta/d\phi_\alpha$. It is seen that only the relative phase, θ , and not the individual phases, is important. Thus, the phase equations can be reduced to one single

differential equation. As seen from Eq. (4), this relative phase is important as it shows in which direction the power flows. If the relative phase is positive, the power is transferred from the pumps to the signal and idler, whereas if it is negative, the opposite happens. As power is transferred from the pumps to the signal and idler, nonlinear detuning occurs, which reduces the coupling. At some point the relative phase can be changed so much that the power flow is reversed and the power begins to couple back to the pumps.

Because the parametric process is symmetric, the signal and the idler have the same increase in power (photon flux), whereas the pumps have the same decrease, also written as $d_z(P_s - P_i) = 0$ and $d_z(P_2 - P_3) = 0$. Finally, the process is power conserving, so $\sum_{\alpha} P_{\alpha}(z) = P_{total}$. Because of these facts, all the powers are related to each other, and can thus be described by only one variable according to the Manley-Rowe relations [18, 19]. This variable, F , is chosen to be the power of the idler which is assumed zero at $z = 0$, i.e.

$$P_1 = P_s + F, \quad (6a)$$

$$P_2 = P_3 = P_p - F, \quad (6b)$$

$$P_4 = F, \quad (6c)$$

where P_s is the input power of the signal, and P_p is the input power for each of the two pumps. These relations reflect the facts that pump photons are destroyed in pairs and sideband photons are created in pairs, or *vice versa*. With this change of notation, the gain of the signal is found to be

$$G(z) = \frac{P_s(z)}{P_s(0)} = 1 + \frac{F(z)}{P_s}. \quad (7)$$

From Eq. (6), two governing differential equations can be set up for the power, F , and phase, θ . Specifically,

$$\frac{dF}{dz} = 4\gamma(P_p - F)\sqrt{F(P_s + F)}\sin\theta, \quad (8)$$

$$\begin{aligned} \frac{d\theta}{dz} = & 2\gamma \left[(P_p - F) \left(\sqrt{\frac{F}{P_s + F}} + \sqrt{\frac{P_s + F}{F}} \right) - 2\sqrt{F(P_s + F)} \right] \cos\theta \\ & + \gamma\delta - 4\gamma F, \end{aligned} \quad (9)$$

where

$$\delta = \frac{\Delta\beta}{\gamma} + 2P_p - P_s. \quad (10)$$

This effective phase mismatch also includes the signal power, which in the quasi-linearized case is omitted due to the assumptions made. The two differential equations have the Hamiltonian

$$H = 4\gamma(P_p - F)\sqrt{F(P_s + F)}\cos\theta + \gamma(\delta - 2F)F. \quad (11)$$

This was found by using a qualified guess and knowing it has to fulfill Hamilton's equations

$$\frac{dF}{dz} = -\frac{\partial H}{\partial \theta}, \quad \frac{d\theta}{dz} = \frac{\partial H}{\partial F}. \quad (12)$$

The first term on the RHS of Eq. (11) is due to FWM, while the second contains the linear and nonlinear phase-modulation terms. Because the Hamiltonian is independent of z , it is constant.

It is therefore used to reduce the problem to one variable. Since F is initially zero, the value of the Hamiltonian is also zero. Thus, the phase, θ , can be determined as

$$\cos \theta = \frac{-(\delta - 2F)F}{4(P_p - F)\sqrt{F(P_s + F)}}. \quad (13)$$

From Eq. (8) a potential equation may be obtained for F , by squaring the equation and inserting the expression for θ , resulting in

$$\left(\frac{dF}{dz}\right)^2 = \gamma^2 \left[16(P_p - F)^2 F(P_s + F) - (\delta - 2F)^2 F^2 \right]. \quad (14)$$

For any given value of the wave-number mismatch, this can be written as

$$\left(\frac{dF}{dz}\right)^2 = 12\gamma^2 F(f_1 - F)(f_2 - F)(F - f_3), \quad (15)$$

where f_j , $j \in (1, 2, 3)$, are the roots of the polynomial and $f_1 \geq f_2 > F(0) > f_3$. The ordering of these roots is important because it affects the structure of the solution. The solution for F will be bounded by the roots of the potential equation. The lower boundary is zero, and the upper boundary is the root f_2 . The value of this root will thus be the maximal value of the power added to both the signal and the idler. The potential equation can be solved using Jacobi elliptic functions [20]. The solution is

$$F(z) = \frac{f_3 f_2 \operatorname{sn}^2 \left[\gamma z \sqrt{3f_1(f_2 - f_3)}, m \right]}{-f_2 + f_3 + f_2 \operatorname{sn}^2 \left[\gamma z \sqrt{3f_1(f_2 - f_3)}, m \right]}, \quad (16)$$

where sn is an elliptic function and the squared modulus

$$m^2 = \frac{f_2(f_1 - f_3)}{f_1(f_2 - f_3)}. \quad (17)$$

It is possible to achieve complete power conversion from the pumps to the signal and idler. In this case the power of the idler equals the initial power of the pumps, thus $F = P_p$. When inserted into the Hamiltonian, knowing that the value of the Hamiltonian is zero, one sees that complete power conversion requires that $\delta = 2P_p$, giving a wave-number mismatch of

$$\Delta\beta = \gamma P_s. \quad (18)$$

This differs significantly from the usually desired value of $-2\gamma P_p$ which results in the initially fastest growing signal. From Eq. (2), the initial growth rate for $\Delta\beta = -2\gamma P_p$ is $G(z) = 1 + \sinh^2 [2\gamma P_p z]$, whereas the growth rate for $\Delta\beta = \gamma P_s$ is $G(z) \approx 1 + \frac{4}{3} \sinh^2 [\sqrt{3}\gamma P_p z]$. With $\Delta\beta = \gamma P_s$, the roots of Eq. (9) are $f_1 = f_2 = P_p$ and $f_3 = -4P_s/3$. In this case, $m = 1$, reducing the elliptic function, sn , to the hyperbolic tangent function, \tanh . The solution is thus rewritten as

$$F(z) = \frac{4P_p P_s \sinh^2 \left[\gamma z \sqrt{P_p(3P_p + 4P_s)} \right]}{3P_p + 4P_s + 4P_s \sinh^2 \left[\gamma z \sqrt{P_p(3P_p + 4P_s)} \right]}. \quad (19)$$

In the interval $-6\gamma P_p < \Delta\beta < 2\gamma P_p$, in which g is a real parameter, approximate solutions to the roots of Eq. (14) are found by treating P_s as a small perturbation to the potential equation.

The three non-zero roots are

$$r_a = -16P_s \frac{P_p^2}{\left(P_p + \frac{1}{6} \frac{\Delta\beta}{\gamma}\right) \left(P_p - \frac{1}{2} \frac{\Delta\beta}{\gamma}\right)}, \quad (20a)$$

$$r_b = P_p + \frac{1}{6} \frac{\Delta\beta}{\gamma} - 12P_s \frac{P_s - \frac{\Delta\beta}{\gamma}}{2P_p - \frac{\Delta\beta}{\gamma}}, \quad (20b)$$

$$r_c = P_p - \frac{1}{2} \frac{\Delta\beta}{\gamma} - 4P_s \frac{3P_p + 2 \frac{\Delta\beta}{\gamma}}{6P_p + \frac{\Delta\beta}{\gamma}}. \quad (20c)$$

The first root, r_a is the lowest root, thus it is equivalent to f_3 , and it is seen that this root is proportional to $-P_s$. The other two roots are equivalent to f_1 and f_2 . However, as r_b is not always greater than r_c , it will depend on the values of $\Delta\beta$, which root is equivalent to which f . It is important to notice that they are both proportional to P_p . Therefore, under the assumption that $P_p \gg P_s$, $m \approx 1$, the elliptic function sn can be approximated with \tanh for small values of z . Thus, the solution can be expressed as

$$F(z) \approx \frac{\frac{-f_2 f_3}{f_2 - f_3} \sinh^2 \left[\gamma z \sqrt{3f_1(f_2 - f_3)} \right]}{1 + \frac{1}{f_2} \frac{-f_2 f_3}{f_2 - f_3} \sinh^2 \left[\gamma z \sqrt{3f_1(f_2 - f_3)} \right]}. \quad (21)$$

For very small values of z , the second term in the denominator can be neglected, reducing it to an expression similar to Eq. (3). Consequently, we may apply the relations

$$\sqrt{3f_1(f_2 - f_3)} \approx \frac{g}{\gamma}, \quad (22)$$

$$-\frac{f_2 f_3}{f_2 - f_3} \approx P_s \left(\frac{2\gamma P_p}{g} \right)^2, \quad (23)$$

which, for the interval $-4\gamma P_p < \Delta\beta < \gamma P_p$, have a relative error of less than 1% for $P_s = 0$ dBm, and this error decreases as the input power decreases. With this approximation, F may be expressed as

$$F(z) \approx \frac{F_{QL}(z)}{1 + \frac{F_{QL}(z)}{P_{sat}}} = P_s \frac{\left[\frac{2\gamma P_p}{g} \sinh^2(gz) \right]^2}{1 + \frac{P_s}{P_{sat}} \left[\frac{2\gamma P_p}{g} \sinh^2(gz) \right]^2}, \quad (24)$$

where $g^2 = (2\gamma P_p)^2 - (\kappa/2)^2$, $\kappa = 2\gamma P_p + \Delta\beta$, and

$$P_{sat} = f_2 \approx \begin{cases} \frac{1}{6} \left(\frac{\Delta\beta}{\gamma} - P_s \right) + P_p, & -6P_p < \frac{\Delta\beta}{\gamma} < P_s, \\ -\frac{1}{2} \left(\frac{\Delta\beta}{\gamma} - P_s \right) + P_p, & P_s < \frac{\Delta\beta}{\gamma} < 2P_p. \end{cases} \quad (25)$$

This final expression for F is a simple expression, using the quasi-linearized result to create an expression that includes the saturation of the pumps. P_{sat} is the upper limit of the power that can be coupled into the idler. From this it is also clear that using a linear mismatch that equals the nonlinear wave-number shift of the signal, γP_s , enables complete power transfer from the pumps into the signal and idler, whereas using a linear mismatch that equals the nonlinear wave-number shift of the pump, i.e. $\Delta\beta = -2\gamma P_p$, can only convert about 67%. However, in the latter case the initial coupling efficiency is higher.

If the two pumps have different powers, called P_a and P_b , where $P_a > P_b$, then $(P_p - F)^2$ is replaced by $(P_a - F)(P_b - F)$ in Eq. (14), and $2P_p$ is replaced by $P_a + P_b$ in Eq. (10). When these changes are made, the solution is the same as Eq. (16). Because of the different pump powers, the wave-number mismatch that results in full power transfer from the weaker pump is $\Delta\beta = \gamma P_s + \gamma(P_a - P_b)$, whereas the fastest growing gain condition is $\Delta\beta = -\gamma(P_a + P_b)$.

3. Discussion

To show the validity of the proposed model, the evolution of the idler as predicted by Eq. (24) has been plotted in Fig. 1 against the full solution, described by Eq. (16), as well as against the quasi-linearized model, Eq. (2). From the figure it is seen that the new expression fits well until the power begins to couple back into the pump. In all cases the new approximate expression has a better correlation with the analytic solution than the conventional quasi-linear result in Eq. (2).

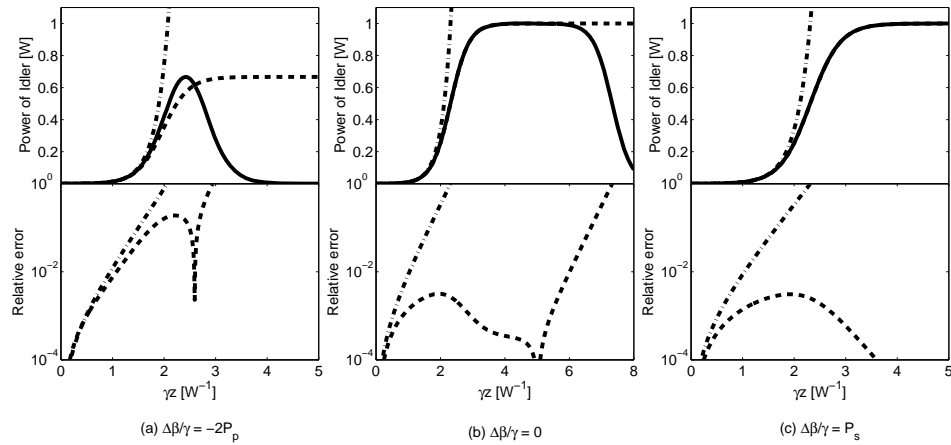


Fig. 1. Evolution of the power of the idler with $P_p = 30$ dBm and $P_s = 0$ dBm. The solid line shows the full analytic solution, the dash-dotted line is the usual quasi-linearized solution and the dashed line is the approximate solution found in this paper. It is evident that the setup in (c) results in complete power transfer, whereas the usual desired setup (a) results in the fastest growing idler. (b) shows that a zero wave-number mismatch results in an almost complete power transfer.

Figure 2 shows the gain for different input powers. The gain has been evaluated by using Eqs. (2), (21) and (24) and it also shows that the new approximation, Eq. (24), is a better approximation to Eq. (21) than the usual approximation, Eq. (2). The new approximation takes saturation into account, but since it does not include back coupling, it is only useful until back coupling becomes significant. Before the system is in depletion, the gain is symmetric around $\kappa = 0$ as predicted by Eq. (2), but when saturation sets in, the gain profile becomes asymmetric which the new approximation also takes into account. If a setup is constructed with two pumps placed symmetrically around the ZDW, then it is possible to obtain a flat gain spectrum over a range of wavelengths, with very high signal gain. The wave-number mismatch is estimated by Taylor expanding all the propagation constants around the ZDW. Because of the chosen pump symmetry, all $\beta_n = d^n\beta(\omega)/d\omega^n|_{\omega_{\text{ZD}}}$, where n is odd, will cancel out, and since β_2 is zero at the ZDW, the first term that has influence is β_4 . The mismatch is thus approximated as

$$\Delta\beta \approx \frac{\beta_4}{12} [(\omega_s - \omega_{\text{ZD}})^4 - (\omega_p - \omega_{\text{ZD}})^4]. \quad (26)$$

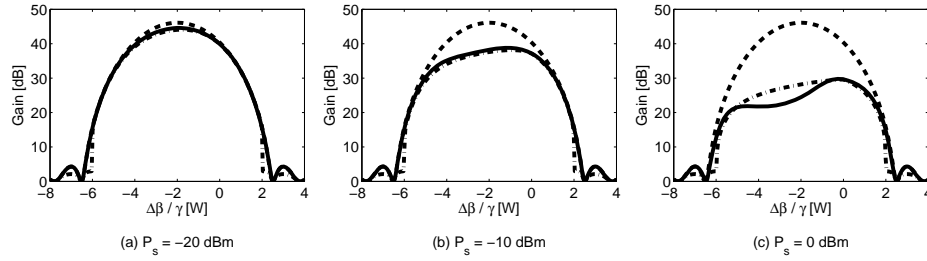


Fig. 2. Gain calculated at $\gamma L = 3 \text{ W}^{-1}$ with $P_p = 30 \text{ dBm}$. The solid line is the analytically calculated gain, the dashed line is the gain calculated from Eq. (2) and the dash-dotted line is calculated using the approximations described in this paper. In (a) the pumps are not in saturation, so there is no significant difference between them. However, in (b) the pumps begin to be in saturation, which Eq. (2) does not take into account. In (c) the input power is so high that the pumps have depleted and for some values of $\Delta\beta/\gamma$ the power has started to couple back into the pumps resulting in lower gain. Only the full analytic solution accounts for this phenomenon.

β_4 can obtain both positive and negative values, depending on the chosen fiber [21], but to get a uniform gain over a wide range, the important factor will be to have β_4 as close to zero as possible, which allows the mismatch to be maintained close to zero over a large bandwidth. This is demonstrated in Fig. 3, which shows gain profiles for a highly nonlinear fiber (HNLF), [6], with $L = 250 \text{ m}$, $\lambda_{\text{ZDW}} = 1560.5 \text{ nm}$, $\beta_4(\lambda_{\text{ZDW}}) = 8.82 \times 10^{-55} \text{ s}^4/\text{m}$ and $\gamma = 11.5 \text{ W}^{-1}\text{km}^{-1}$, calculated using Eq. (24). If Eq. (1) is solved numerically and a loss of 0.74 dB/km is included, the obtained spectrum is similar to that shown in Fig. 3, only the gain is lower by 1.5 to 2 dB . It

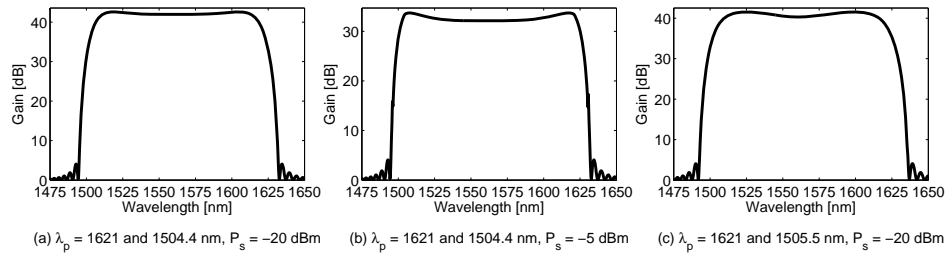


Fig. 3. Gain profiles for 30-dBm pumps. For cases in which the pumps are placed symmetrically around the ZDW, as in (a) and (b), it is seen that the gain is wide and flat over 113 and 123 nm for the undepleted (a) and depleted (b) case, respectively. It is possible to slightly misalign one of the pumps and continue to have wide and flat gain (c).

is important for the pumps to be placed far from the ZDW, in this case a separation of roughly 60 nm was used, in order to avoid the creation of extra waves by cascaded FWM [22], which invalidate the approximation of only 4 distinct frequencies. Furthermore, simulations show that when the signal is placed relatively close to either of the pumps, then the coupling efficiency is greatly reduced because the signal undergoes degenerate FWM with the nearer pump. For this fiber setup, degenerate FWM begins to be significant at a separation of roughly 10 nm . This effect reduces the actual obtainable bandwidth.

In Fig. 3, it is also shown that even if the symmetry is slightly broken, the gain spectrum remains reasonably flat, and its width even increases slightly.

4. Conclusion

We have obtained the exact solution of the dual-pumped FOPA equations, as well as a simple, yet very useful, approximate solution which includes pump depletion and nonlinear detuning. We have shown with a concrete example, which shows that it is possible to obtain flat gain bandwidths in the 100-nm range, that the model provides a simple and fast way of modeling the gain of a FOPA.

We have also shown that although the gain increases more rapidly as a function of fiber length when $\Delta\beta = -2\gamma P_p$, this wave-number mismatch does not result in complete power conversion, as is the case when $\Delta\beta = \gamma P_s$.

Acknowledgments

EOARD is thanked for financial support under grant number 063094. Magnus Karlsson is acknowledged for fruitful discussions.